Solution electrostatics beyond pH: a coarse grained approach to ion specific interactions between macromolecules

Kurut Sabanoglu, Anil; Lund, Mikael

Published in:
Faraday Discussions

DOI:
10.1039/c2fd20073b

2013

Faraday Discussions Vol 160

Ion Specific Hofmeister Effects

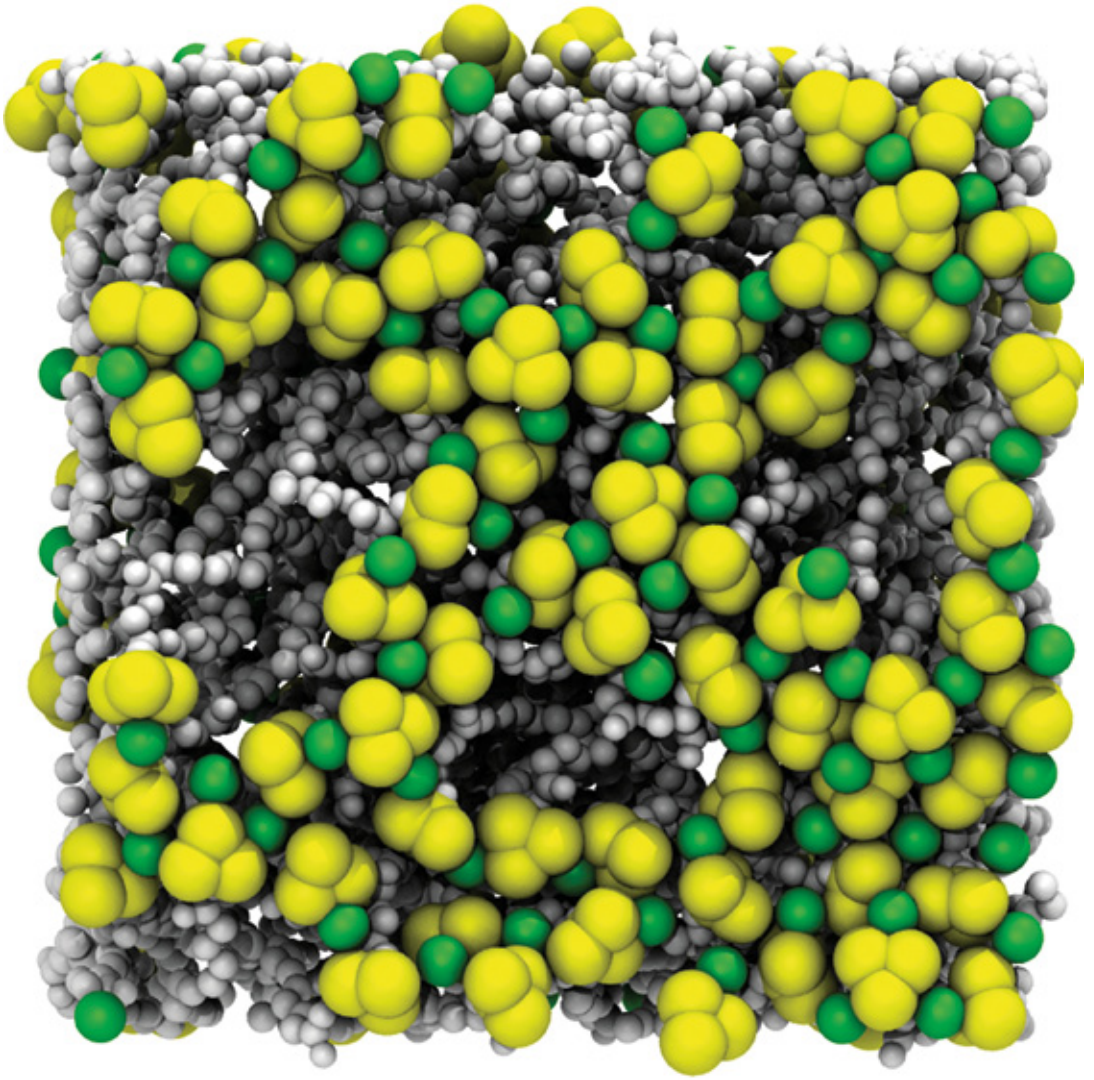

RSC Publishing

Solution electrostatics beyond pH: a coarse grained approach to ion specific interactions between macromolecules

Anıl Kurut* and Mikael Lund*

Received 13th April 2012, Accepted 10th May 2012
DOI: 10.1039/c2fd20073b

Oblivious to ion specificity, pH has been a key parameter for macromolecular solutions for little more than a century. We here widen the concept by describing the ionization of macromolecules not only *via* pH, but also pX where X are other binding species. Using binding constants, measured by NMR, of chloride and thiocyanate to amino acid motifs on γ-crystallin, we calculate i) titration curves as a function of pH and pX and ii) estimate second virial coefficients using both approximate theory and computer simulations. In agreement with experiment, a Hofmeister reversal for protein–protein interactions is observed when crossing iso-electric conditions. Thiocyanate binding further leads to large charge fluctuations that may trigger intermolecular charge regulation interactions.

1 Introduction

For nearly a century, chemists and other natural scientists have been brought up with concepts such as pH, Brønsted acids and bases, auto-protolysis, and pK_a-values. This terminology focuses on thermodynamic equilibrium processes of merely a single ionic species, namely *protons*. pH is hence a key parameter throughout a number of scientific disciplines and is commonly used as a convenient handle to control inter- and intra-molecular electrostatic interactions. Protons are, however, not alone. Plenty of other ions may be present, yet our standard terminology is unable to account for those. During the last two decades there has been a large development in the molecular understanding of ion specific effects; the reader may refer to recent reviews for a full account.[1–3] It has for example long been known that proteins can be titrated with anions and that this changes the thermodynamic properties,[4–6] yet only recently have the underlying molecular mechanisms started to unravel. Experimental and theoretical works both show that small and large anions distinctly distribute on molecular surfaces; large anions bind to non-polar motifs[7–11] and thiocyanate, for example, binds to the backbone of model peptides.[12] The binding affinities to molecular motifs are currently being systematically quantified[12,13] and an obvious question is if specific ion binding can be treated at the same level as protons have been for so long. That is, through the chemical potential (*cf.* pH) and binding equilibrium constant to molecular motifs (*cf.* pK_a values) we may reduce the microscopic ion-motif potential of mean force to a two state binding model:

$$\mathrm{MX} \rightleftharpoons \mathrm{M} + \mathrm{X} \tag{1}$$

where M is the motif and X is the ion in question. Arguably, protons distinguish themselves from other ions in that they are always present in water and their binding

Department of Theoretical Chemistry, Lund University, P.O.B. 124, SE-22100 Lund, Sweden. E-mail: anil.kurut@teokem.lu.se; mikael.lund@teokem.lu.se; Tel: +46 462 223167

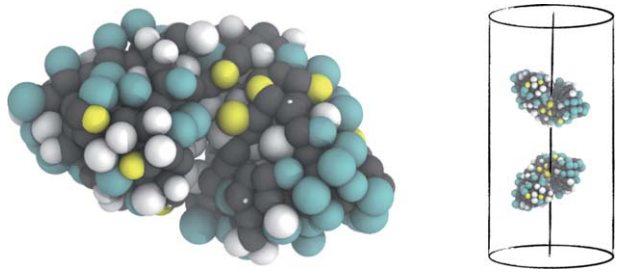

Fig. 1 Left: protein model used in the Monte Carlo simulations. Protons can bind to acidic and basic sites (turquoise); thiocyanate may bind to the backbone (black) as well as to hydrophobic side chains (yellow). Right: two-body simulation model in a cylindrical container – solvent and salt are handled implicitly.

is of covalent nature. This is fitting for a two-state model as the configurational space may readily be divided into a well defined bound and unbound state. This (arbitrary) division becomes more difficult for weakly bound ions, yet formally a thermodynamic binding constant can always be defined, provided that the ion-motif potential of mean force has a distinct minimum and decays with distance, r, as $1/r^3$ of faster.[14] The mere fact that a binding constant can be reliably measured, preferably with different experimental techniques, of course also supports a two-state model.

In this work we present a coarse grained model for macromolecules in solution, taking into account specific ion binding to dedicated molecular motifs. The model is based on continuum electrostatics, combined with two-state binding of protons and an arbitrary number of other ions. Ultimately this allows for studies of ion specific effects at large length scales hitherto unattainable with existing models.

2 Model and theory

2.1 Simulation model

Solvent and salt particles are treated at the Debye–Hückel level while the rigid proteins are described in mesoscopic detail where each amino acid is represented by two soft spheres: one for the backbone and another for the side chain – see Fig. 1. These spheres are placed at their respective mass centers as found in the atomistic NMR or crystal structure and their radii are determined from the atomic weight, assuming a density of 1 g ml^{-1}. To capture specific ion binding to the macromolecular surface we specify binding sites (Table 1) where the free energy difference between the bound and free state is $k_B T \ln 10(\mathrm{pX} - \mathrm{p}K_d)$. Analogous to pH, pX is the minus logarithm of the activity† of the binding ion, X, and K_d is the dissociation constant for the process. In addition to electrostatic and van der Waals pair interactions, hydrophobic side-chains interact with a square-well potential and the final system Hamiltonian becomes:

$$\beta U = \sum_{i\neq j}^{N} \frac{\lambda_B z_i z_j e^{-\kappa r_{ij}}}{r_{ij}} + \sum_{i\neq j}^{N} 4\beta\varepsilon_{LJ}\left[\left(\frac{\sigma_{ij}}{r_{ij}}\right)^{12} - \left(\frac{\sigma_{ij}}{r_{ij}}\right)^{6}\right] + \sum_{i\neq j}^{N_{\mathrm{hydroph.}}} \beta u_{sw} + \sum_{i\neq j}^{N_{\mathrm{bound}}} (\mathrm{pX}_i - \mathrm{p}K_{d,i}) \ln 10 \quad (2)$$

where the first two sums run over all particles, the third over hydrophobic side chains and the last term over sites with bound ions, only. $\lambda_B = 7.1$ Å is the Bjerrum length

† In this work we assume that the activity is equal to the concentration.

Table 1 Amino acid properties and binding sites of γD-crystallin (PDB: 2KLJ[16]). Only particles with solvent accessible surface area (SASA) larger than 30 Å^2 are included as ion binding sites; this is indicated by parenthesis in the *N* column. When ions bind to a hydrophobic site, this is rendered non-hydrophobic. A probe with radius 1.4 Å is used in SASA measurements

Atom type	*N*	σ/Å	pK_{d,H^+}	$pK_{d,\ SCN^-}$[12]	Hydrophobic
Asp	12 (10)	4.8	4.0		no
Glu	10 (9)	5.2	4.4		no
His	6 (4)	5.4	6.3		no
Tyr	14 (7)	5.9	9.6		no
Lys	1 (1)	5.2	10.4		no
Cys	6 (0)	4.5	10.8		no
Arg	21 (21)	5.8	12.0		no
Ctr	1 (1)	4.7	2.6		no
Ntr	1 (1)	4.7	7.5		no
Ala	4 (0)	3.1		0.82	yes/no
Ile	6 (0)	4.8		0.82	-//-
Leu	17 (3)	4.8		0.82	-//-
Met	4 (3)	5.2		0.82	-//-
Phe	6 (1)	5.6		0.82	-//-
Pro	4 (4)	4.3		0.82	-//-
Trp	4 (0)	6.3		0.82	-//-
Val	6 (0)	4.3		0.82	-//-
Ser	17	3.9			no
Thr	4	4.4			no
Asn	7	5.6			no
Gln	11	5.2			no
Gly	14	1.2			no
backbone	156 (5)	4.7		0.60	no
backbone (Pro, Gly)	18 (3)	4.7		1.30	no

for water, z are particle charge numbers, r_{ij} the distance between the i'th and j'th particle, $1/\kappa = 3.04/\sqrt{C_s}$ Å is the Debye screening length,[15] C_s the molar 1 : 1 salt concentration, $\beta = 1/k_B T$ is the inverse thermal energy, and $\beta u_{sw} = -0.8$ for surface separations less than 1.4 Å – zero otherwise. Finally, $\sigma_{ij} = (\sigma_i + \sigma_j)/2$ is the Lennard–Jones diameter and $\beta\varepsilon_{LJ} = 0.088$.

Using Metropolis Monte Carlo (MC) simulations[17] we simulate either one or two of the proteins in a cylindrical container and average over i) mass center positions (fixed along the main axis of the cylinder), ii) orientations, and iii) ion binding states. Translations and rotations for two-body simulations, only, are performed in a combined MC move where a random displacement vector and angle is used to generate configurations in the canonical ensemble. Averaging over ion binding states is done by swap moves where the state of randomly chosen binding sites – see Table 1 – is alternated between bound and unbound. "Bound" simply means that the site charge is changed by $+1e$ or $-1e$ for proton and anion binding, respectively. Ion binding to a hydrophobic group renders the group non-hydrophobic, thus excluding it from hydrophobic interaction. All simulations were performed using the Faunus project.[18]

2.2 Charge regulation

Charge binding sites on molecular surfaces give rise to a fluctuating molecular charge distribution that can be perturbed by an external electric potential. This leads to a correlation effect, known as charge regulation or "fluctuation forces", that lowers the system free energy.[19,20] The mechanism is well known for proton binding

sites, yet for other ions it is largely unexplored and we therefore give a brief overview.

Consider an unperturbed macromolecule with a fluctuating charge distribution with a charge valency, Z, that occurs with the intrinsic probability $P(Z)$. Exposing the molecule to an external electric potential, φ, due to the surrounding chemical environment, the charge ensemble average becomes,

$$\langle Z\rangle = \frac{\int P(Z)Z\exp(-\beta\varphi eZ)\mathrm{d}Z}{\int P(Z)\exp(-\beta\varphi eZ)\mathrm{d}Z}. \tag{3}$$

It then follows that,

$$-\frac{\partial\langle Z\rangle}{\beta e\partial\varphi} = \langle Z^2\rangle - \langle Z\rangle^2 \equiv C. \tag{4}$$

where we have introduced the charge capacitance, C, which is simply the variance of the mean charge.[21] If φ stems from another fluctuating charge distribution, $P(Z')$, the two distributions have the interaction free energy,

$$\beta w(R) = -\ln\int_{-\infty}^{\infty}\int_{-\infty}^{\infty} P(Z)P(Z')\exp\left(-\lambda_B ZZ'/R\right)\mathrm{d}Z\mathrm{d}Z' \approx \frac{\lambda_B\langle Z\rangle\langle Z'\rangle}{R} - \frac{\lambda_B^2}{2R^2}\left(C\langle Z'\rangle^2 + C'\langle Z\rangle^2 + CC'\right) \tag{5}$$

where R is the center–center distance between the two distributions and in the last step we have assumed that P, P' are normal distributions. The same result can be obtained using a multipole expansion[20–22] and the first term is clearly the monopole–monopole interaction term, while the remaining attractive terms are monopole-induced and induced-induced monopole interactions. For the sake of simplicity we do not discuss angular dependent terms and further note that these decay faster than the above terms – $1/R^4$ and $1/R^6$ for monopole–dipole and dipole–dipole interactions, respectively.[23]

Thus, in the intermolecular interaction energy given by eqn (5), electrostatics are condensed to two molecular parameters, i) the average net charge, $\langle Z\rangle$ and ii) the charge capacitance, C. The latter property is central for describing charge regulation phenomena[21] and entails the overall fluctuation effect of all binding ions and thus depends on solution conditions, structure and protein sequence.

2.3 Osmotic second virial coefficient

Through eqn (5), the protein net charge and capacitance can be used to estimate the osmotic second virial coefficient of protein solutions using,

$$B_2 = \frac{2\pi\sigma^3}{3} - 2\pi\int_{\sigma}^{\infty}\left(e^{-\beta}w(R) - 1\right)R^2\mathrm{d}R \tag{6}$$

where the first term, B_2^{HS}, is a simple hard sphere contribution for σ smaller than protein–protein contact, $\sigma = 25$ Å. To take into account the effect of salt screening, λ_B in eqn (5) is replaced with[15]

$$\lambda_B\exp[-\kappa(R - \sigma)]/(1 + \kappa\sigma) \tag{7}$$

where we note that the quadratic charge regulation terms are subject to stronger salt screening than the direct monopole–monopole term.

3 Results and discussion

3.1 Binding of protons, chloride, and thiocyanate

The overall electrostatic properties of bio-molecules are traditionally classified from the pH titration curve, *i.e.* the net charge as a function of the proton activity (pH). To describe how these properties are influenced by additional ions, further dimensions must be added to the titration curve: one for each additional binding species. In the following we assume that the salt cation does not bind to the protein surface, although this could easily be included by expanding Table 1; the computational cost would be negligible.

Fig. 2, top, shows the net charge of γ-crystallin in the presence of chloride and thiocyanate, respectively. Due to weak binding at moderate salt concentrations[5,12,24] we shall assume that chloride interacts only through double layer forces, that is through the Debye screening length. The iso-electric point, pI where the net-charge is zero, thus remains constant over a large span of salt concentrations and the classical one-dimensional pH picture thus gives a good description of the electrostatic properties. For pH ≠ pI the net charge does however change with salt concentration due to screening of intramolecular electrostatic interactions. At high ionic strengths the protein can hence accommodate a higher net-charge, while if $\langle Z \rangle = 0$, screening has little effect since the internal electrostatic energy, roughly proportional to $\langle Z \rangle^2$, is near a minimum.

In contrast, the strongly bound thiocyanate ion behaves very differently. Changing the salt concentration from 30 mM to 300 mM causes a drop in the iso-electric point from nine to five because the increased salt activity drives anion adsorption to the backbone and side-chain binding sites. This process is further aided by the positive net-charge of the protein at low pH, although at sufficiently high salt concentrations the binding sites saturate while at the same time the favorable electrostatic interactions diminish due to screening.

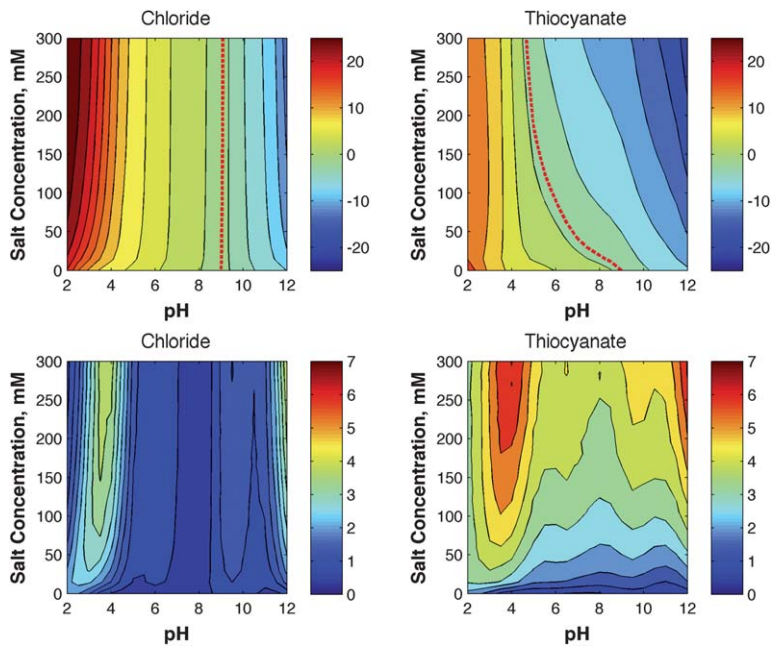

Fig. 2 Protein net charge (top) and charge capacitance (bottom) for γ-crystallin in NaCl (left) and NaSCN (right). The dashed lines on the charge plots represent the iso-electric conditions.

The charge capacitance, C, describes the protein's ability for charge regulation. In the chloride solution, the capacitance is influenced by salt only through the ionic strength; the proton concentration causes maxima at high and low pH, corresponding to the pK_d of acidic and basic sites. As the salt concentration increases the electrostatic interactions between sites are screened and whereby they become independent of each other. In the limit of infinite salt, the capacitance approaches an ideal value, given by[21]

$$C^{\text{ideal}} = \sum_i \frac{10^{pX_i - pK_{d,i}}}{(1 + 10^{pX_i - pK_{d,i}})^2} \tag{8}$$

where the sum runs over all binding sites. Compared to the capacitance where sites interact, the ideal curve tends to be larger in magnitude and hence less broad.

Thiocyanate also here displays a remarkably different picture compared to chloride and, overall, the capacitance is higher in magnitude for all salt and pH conditions. This is trivially due to the added number of binding sites that allows for more charge fluctuations. Increasing the thiocyanate concentration leads to higher capacitances that approach the ideal value as given by eqn (8) and may potentially result in strong charge regulation interactions with other molecular matter. However, as already mentioned, the quadratic charge regulation terms in eqn (5) are screened with $\sim e^{-2\kappa r}$ compared to $\sim e^{-\kappa r}$ for the direct charge–charge term and hence diminish rapidly with increasing salt. Still, thiocyanate causes capacitances several times higher than chloride even at low salt concentrations and the addition of binding ions may hence be a useful tool to tune intermolecular interaction mechanisms, charge regulation in particular.

3.2 Protein–protein interactions

3.2.1 Virial coefficients. In the previous section we discussed the electric properties of γ-crystallin using the average charge, $\langle Z \rangle$, and capacitance, C, while considering both protons and binding anions. Using these isotropic terms we now estimate the osmotic second virial coefficient, B_2, using eqn (5) and eqn (6). As shown in Fig. 3, B_2 for both SCN^- and Cl^- reaches minima for pH close to the iso-electric points, while at extreme pH the net charge of the protein causes a high (repulsive) virial coefficient. Note that B_2 here does not become negative due to the dominance of the repulsive first term in eqn (5) and that we have neglected attractive short ranged van der Waals contributions.

It is instructive to investigate the B_2 *difference* between the NaSCN and NaCl solutions – see Fig. 3, right. At near iso-electric conditions, ΔB_2 is zero and thus marks a reversal of the Hofmeister series. That is, when the protein has

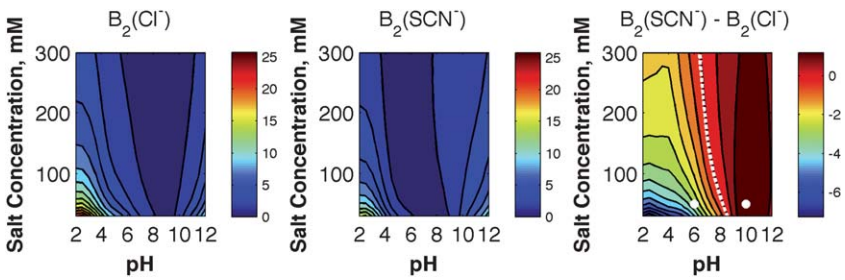

Fig. 3 Left and middle: estimated virial coefficients for γ-crystallin in NaCl and NaSCN, respectively using eqn (5) and eqn (6). Right: difference in second virial coefficient between NaSCN and NaCl. The dashed white line represents zero (Hofmeister reversal), while the two white dots mark the conditions used for the two-body simulations in Fig. 4. Note that the B_2 values are normalized with B_2^{HS}.

a net positive charge, bound thiocyanate anions lower the protein–protein repulsion more than chloride; the *reverse* Hofmeister series.[25] For a net negatively charged protein, binding of thiocyanate causes more repulsion than chloride, *i.e.* the *direct* Hofmeister series. This is exactly what is found in SAXS measurements for γ-crystallin as well as other proteins.[26] Experimentally, the inversion for γ-crystallin occurs at pH 4.5 and at 500 mM salt[26] which is lower than the iso-electric point in dilute solution (pI 6.7–8.9)[26,27] and thus fits the picture that addition of binding salts down shifts pI, *cf.* Fig. 2. While the low salt Hofmeister reversal predicted here also agrees with previous theoretical observations[8,28,30] the current work is distinguished in that ion binding adheres to the complex surface topology of the protein, while at the same time no explicit ions are required.

3.2.2 Two-body simulations. In the previous section we used perturbation theory to estimate the second virial coefficient of γ-crystallin solutions and crudely neglected anisotropy due to electrostatics, van der Waals and excluded volume. This can be remedied by instead explicitly simulating two coarse grained proteins (Fig. 1, right) and from the radial distribution function, $g(R)$, extracting the potential of mean force, $\beta w(R) = -\lg(R)$. As shown in Fig. 4 the protein–protein attraction is larger for thiocyanate anions than chloride anions at pH 6, while the reverse is true at pH 10. This result is in qualitative agreement with the simplistic multipole calculations in Fig. 3, and more elaborate computer simulations with explicit ions,[8] as well as with experimental data.[26] Note also, that there are now distinct minima in the interaction free energies, stemming mostly from van der Waals interactions and, to a lesser extent, hydrophobic interactions *cf.* eqn (2).

4 Conclusion

Using a simple theoretical model that combines ion binding equilibria to macromolecular motifs with continuum electrostatics, we have investigated ion specific charge properties of the protein γ-crystallin. In particular we note that the iso-electric "point" of the protein in thiocyanate solution varies strongly with the salt concentration and is thus a function of both pH and pSCN. Osmotic second virial coefficients – calculated both from a multipole expansion and from two body computer simulations – show a reverse salting-in Hofmeister series for the cationic protein while the direct Hofmeister series is followed under anionic conditions. This is in agreement with SAXS measurements as well as with other theoretical work. While our model accounts for salting in effects, salting out due to highly solvated ions is

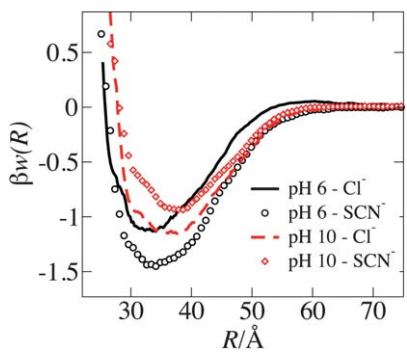

Fig. 4 Simulated potential of mean force, $w(R)$, along the protein–protein mass center coordinate, R, at different pH and anionic species (50 mM). Note the Hofmeister reversal going from low to high pH.

neglected. This may be remedied by introducing salt sensitive hydrophobic interactions;[29] a simple surface tension argument could be a viable option.

With multiple binding sites on the protein surface, thiocyanate brings about large fluctuations in the molecular charge distribution. This may lead to significant charge regulation phenomena when interacting with other molecular matter and specific ion effects may thus provide yet another handle to control intermolecular interactions.

Acknowledgements

We thank Paul Cremer and Pavel Jungwirth for useful discussions. For financial support we thank the eSSENCE@LU strategic program and the Linneaus Center of Excellence "Organizing Molecular Matter", Lund, Sweden.

References

1 P. Jungwirth and B. Winter, *Annu. Rev. Phys. Chem.*, 2008, **59**, 343–66.
2 Y. Zhang and P. S. Cremer, *Annu. Rev. Phys. Chem.*, 2010, **61**, 63–83.
3 P. Lo Nostro and B. W. Ninham, *Chem. Rev.*, 2012, **112**, 2286–2322.
4 E. Volkin, *Journal of Biological Chemistry*, 1948, **175**, 675–681.
5 P. Retailleau, M. Riès-Kautt and A. Ducruix, *Biophys. J.*, 1997, **73**, 2156–63.
6 K. D. Collins, *Methods (San Diego, Calif.)*, 2004, **34**, 300–11.
7 R. L. Baldwin, *Biophys. J.*, 1996, **71**, 2056–63.
8 M. Lund and P. Jungwirth, *J. Phys.: Condens. Matter*, 2008, **20**, 494218.
9 H. Krienke, V. Vlachy, G. Ahn-Ercan and I. Bako, *J. Phys. Chem. B*, 2009, **113**, 4360–4371.
10 C. Gibb, *J. Am. Chem. Soc.*, 2011, **133**, 7344–7347.
11 E. A. Algaer and N. F. A. van der Vegt, *J. Chem. Phys. B*, 2011, 13781–13787.
12 K. Rembert, J. Paterova, J. Heyda, C. Hilty, P. Jungwirth and P. Cremer, *J. Am. Chem. Soc.*, 2012, **134**, 10039–10046.
13 L. M. Pegram and M. T. Record, *J. Phys. Chem. B*, 2008, **112**, 9428–36.
14 D. F. Evans and H. Wennerström, *The Colloidal Domain - Where Physics, Chemistry, Biology and Technology Meet*, VCH Publishers, New York, 1994.
15 T. L. Hill, *An Introduction to Statistical Thermodynamics*, Dover Publications Inc., New York, 1986.
16 J. Wang, X. Zuo, P. Yu, I.-J. L. Byeon, J. Jung, X. Wang, M. Dyba, S. Seifert, C. D. Schwieters, J. Qin, A. M. Gronenborn and Y.-X. Wang, *J. Am. Chem. Soc.*, 2009, **131**, 10507–10515.
17 N. Metropolis, A. Rosenbluth, M. Rosenbluth, A. Teller, E. Teller and Others, *J. Chem. Phys.*, 1953, **21**, 1087.
18 M. Lund, M. Trulsson and B. Persson, *Source Code Biol. Med.*, 2008, **3**, 1.
19 K. Linderstrøm-Lang, *Compt. Rend. trav. lab. Carlsberg*, 1924, **15**, 1–29.
20 J. G. Kirkwood and J. B. Shumaker, *Proc. Natl. Acad. Sci. U. S. A.*, 1952, **38**, 855–62.
21 M. Lund and B. Jönsson, *Biochemistry*, 2005, **44**, 5722–7.
22 M. L. Grant, *J. Phys. Chem. B*, 2001, **105**, 2858–2863.
23 D. Bratko, A. Striolo, J. Z. Wu, H. W. Blanch and J. M. Prausnitz, *J. Phys. Chem. B*, 2002, **106**, 2714–2720.
24 X. Chen, T. Yang, S. Kataoka and P. Cremer, *J. Am. Chem. Soc.*, 2007, **129**, 12272–12279.
25 Y. Zhang and P. S. Cremer, *Proc. Natl. Acad. Sci. U. S. A.*, 2009, **106**, 15249–53.
26 S. Finet, F. Skouri-Panet, M. Casselyn, F. Bonneté and A. Tardieu, *Curr. Opin. Colloid Interface Sci.*, 2004, **9**, 112–116.
27 S. Zigman, J. Schultz and T. Yulo, *Comp. Biochem. Physiol., Part B: Biochem. Mol. Biol.*, 1983, **75**, 425427.
28 M. Boström, F. W. Tavares, S. Finet, F. Skouri-Panet, A. Tardieu and B. W. Ninham, *Biophys. Chem.*, 2005, **117**, 217–24.
29 M. Jönsson, M. Skepö and P. Linse, *J. Phys. Chem. B*, 2006, **110**, 8782–8.
30 M. Boström, D. F. Parsons, A. Salis, B. W. Ninham and M. Monduzzi, *Langmuir*, 2011, **27**, 9504–9511.

